



# Millennial-age GDGTs in forested mineral soils: $^{14}\text{C}$ -based evidence for stabilization of microbial necromass

Hannah Gies<sup>1</sup>, Frank Hagedorn<sup>2</sup>, Maarten Lupker<sup>1</sup>, Daniel Montluçon<sup>1</sup>, Negar Haghypour<sup>1,3</sup>, Tessa Sophia van der Voort<sup>4</sup>, and Timothy Ian Eglinton<sup>1</sup>

<sup>1</sup>Department of Earth Sciences, ETH Zürich, Sonneggstrasse 5, 8092 Zürich, Switzerland

<sup>2</sup>Swiss Federal Institute for Forest, Snow and Landscape Research WSL, Zürcherstrasse 111, 8903 Birmensdorf, Switzerland

<sup>3</sup>Laboratory of Ion Beam Physics, ETH Zürich, Otto-Stern-Weg 5, 8093 Zürich, Switzerland

<sup>4</sup>Campus Fryslan, Rijksuniversiteit Groningen, Wirdumerdijk 34, 8911 CE Leeuwarden, Netherlands

**Correspondence:** Hannah Gies (hannah.gies@erdw.ethz.ch)

**Abstract.** Understanding controls on the persistence of soil organic matter (SOM) is essential to constrain its role in the carbon cycle and inform climate-carbon cycle model predictions. Emerging concepts regarding formation and turnover of SOM imply that it is mainly comprised of mineral-stabilized microbial products and residues, however, direct evidence in support of this concept remains limited. Here, we introduce and test a method for isolation of isoprenoid and branched glycerol dialkyl glycerol tetraethers (GDGTs) – diagnostic membrane lipids of archaea and bacteria, respectively - for subsequent natural abundance radiocarbon analysis. The method is applied to depth profiles from two Swiss pre-alpine forested soils. We find that the  $\Delta^{14}\text{C}$  values of these microbial markers markedly decrease with increasing soil depth, indicating turnover times of millennia in mineral subsoils. The contrasting metabolisms of the GDGT-producing microorganisms indicates it is unlikely that the low  $\Delta^{14}\text{C}$  values of these membrane lipids reflect heterotrophic acquisition of  $^{14}\text{C}$ -depleted carbon. We therefore attribute the  $^{14}\text{C}$ -depleted signatures of GDGTs to their physical protection through association with mineral surfaces. These findings thus provide strong evidence for the presence of stabilized microbial necromass in forested mineral soils.

## 1 Introduction

Soil organic matter (SOM) represents the largest reservoir of carbon in terrestrial ecosystems, exchanging large quantities of carbon with the atmosphere and supplying aquatic systems with organic and inorganic C (Parry et al., 2007; Battin et al., 2009; Bradford et al., 2016). SOM is comprised of a complex mixture of components that turn over on a wide range of timescales (from seconds to millennia), introducing large uncertainties in climate model predictions (Carvalhais et al., 2014; He and Yu, 2016). Emerging concepts of SOM suggest that only a small fraction of annual C inputs from plants persists in the soils, and that microbial products and residues stabilized by the interaction with reactive minerals comprise the majority of the soil C pool (Schmidt et al., 2011; Cotrufo et al., 2015; Lehmann and Kleber, 2015; Kallenbach et al., 2016; Kästner and Miltner,



2018). Correspondingly, microbial processes are increasingly being incorporated into soil carbon cycle models (Riley et al., 2014; Ahrens et al., 2015). However, evidence of the ‘entombment’ of microbial necromass is presently limited and largely circumstantial, being primarily based on the finding of increasing contributions of microbial biomarker as compared plant-derived compounds with increasing soil depth (Amelung et al., 2008; Miltner et al., 2012; Kallenbach et al., 2016; Liang et al., 2019; Ma et al., 2018).

Radiocarbon provides valuable constraints on carbon turnover in soils (Trumbore et al., 1996; Schrumppf and Kaiser, 2015), and  $^{14}\text{C}$  measurements are particularly useful when applied at the level of specific compounds (e.g., Van der Voort et al., 2017). Prior radiocarbon analyses of plant-derived biomarkers have indicated their stabilization in mineral soils (Huang et al., 1999; van der Voort et al., 2016), but  $^{14}\text{C}$ -based evidence for stabilization of microbial necromass in SOM is currently lacking.  $\Delta^{14}\text{C}$  signatures of fatty acids and phospholipid-fatty acids (PLFAs), established indicators for plant and microbial-derived C, suggest active microbial re-synthesis of lipids in deeper soil (Matsumoto et al., 2007; Gleixner, 2013) rather than the stabilization of microbial necromass (Kramer and Gleixner, 2008).

Here we examine the  $^{14}\text{C}$  characteristics of Glycerol Dialkyl Glycerol Tetraethers (GDGTs) – characteristic membrane lipids of microorganisms that are ubiquitous in terrestrial and aqueous environments (Schouten et al., 2013). GDGTs are subdivided into two groups of compounds: isoprenoid GDGTs (isoGDGTs) produced by Archaea (De Rosa and Gambacorta, 1988) and branched GDGTs (brGDGTs) which are of putative bacterial origin (Weijers et al., 2006a) and are especially abundant in soils and peats (Weijers et al., 2006b)(For molecular structures see Figure A1). GDGTs have garnered much attention due to their potential as molecular proxies for environmental conditions: the relative abundance of branched versus isoprenoid GDGTs has been used to qualitatively estimate soil-derived carbon input into marine sediments (Hopmans et al., 2004), while the internal distribution of iso- and branched GDGT isomers carries information of aquatic and soil conditions (Schouten et al., 2002; Powers et al., 2004, 2010; Liu et al., 2013; Coffinet et al., 2014; Yang et al., 2016). For example, the distribution of different brGDGTs, parameterized as the methylation of branched tetraethers (MBT) and cyclisation of branched tetraethers (CBT) indices (Peterse et al., 2012; De Jonge et al., 2014; Naafs et al., 2017), have been found to correlate with mean annual continental air temperature (MAT) and soil pH Weijers et al. (2007), respectively.

Despite their rapid adoption by biogeochemists and paleoclimatologists as valuable molecular tracers and proxies of carbon source and environmental conditions, there are numerous aspects regarding their production, turnover and fate that remain enigmatic. In particular, despite their ubiquity in soils and other environmental matrices, the biological precursors, metabolic processes and physiological drivers giving rise to brGDGT signatures observed in terrestrial and aquatic systems remain poorly constrained. In this context, natural abundance-level radiocarbon measurements of these compounds may provide a valuable approach to better understand their source(s) and turnover rates, while also shedding light on processes that influence their abundance and distribution.

Prior  $^{14}\text{C}$ -based studies of GDGTs have primarily focused on the isoprenoid compounds in marine waters and sediments (Pearson et al., 2001; Smittenberg et al., 2004; Ingalls et al., 2006; Mollenhauer et al., 2007, 2008; Shah et al., 2008). The only reported investigation of branched GDGT  $^{14}\text{C}$  characteristics in lake sediments (Birkholz et al., 2013) yielded  $\Delta^{14}\text{C}$  values than expected based on the depositional age of the sediment. that were lower than those of the depositional age of the sediment,



although the causes of this pre-aged signal was not established. Although soils are considered a major source of brGDGTs to aquatic systems, the  $^{14}\text{C}$  signatures of brGDGTs in soils has not been determined. Thus, we presently lack crucial information concerning both the production and cycling of this distinctive group of microbial lipids in the context of soil C cycling, as well as the implications for their uses as molecular tracers and proxies.

60 In the present study, we used molecular-level natural-abundance  $^{14}\text{C}$  measurements to constrain the provenance and turnover of GDGTs in soils. We developed and rigorously tested a preparative high performance liquid chromatography (HPLC) method to isolate both isoprenoid and branched GDGTs from soils (and sediments) for subsequent small-scale radiocarbon analysis by accelerator mass spectrometry (AMS). We then applied this method to samples from two well-studied sub-alpine Swiss soil profiles in order to shed light on their origin and stability. As unequivocal markers of microbial contributions to soils, the  
65 GDGTs provide an opportunity to assess the stability and turnover of microbial biomass in soils.

## 2 Methods

### 2.1 Study Site

Soils were sampled by taking soil cores at two forested sites in Switzerland, one near Lausanne (46.5838°N, 6.6580°E, 800 m asl), and the other one close to Beatenberg (46.7003°N, 7.7623°E, 1490 m asl). Both sites are both part of the Long-term Forest  
70 Ecosystem Research (LWF) network (Innes, 1995) maintained by the Swiss Federal Institute for Forest, Snow and Landscape Research (WSL).

The subalpine soil from the site at Beatenberg is a Podzol which has a thick organic layer followed by a 10 cm A-horizon, and carbonate-free sandstone as parent material. The MAT at the site is 4.6°C and the pH rises from 3.7 to 4.4 with increasing soil depth. The second soil from the Swiss Plateau close to Lausanne is a Cambisol developed on top of a carbonate-containing  
75 moraine. Its A-Horizon extends to 50 cm with a total soil depth of 3 m. Here, the MAT is 7.6°C, the pH is slightly higher compared to the Beatenberg soil and largely invariant (4.6 to 4.5) to a depth of 80 cm (Walthert, 2003).

At each site soil cores were sampled following protocols implemented as part of the LWF sampling program (van der Voort et al., 2016). These soil composites have been previously analyzed for radiocarbon signatures of organic carbon in bulk soil and soil density fractions, as well as in specific alkanes and fatty acids (Van der Voort et al., 2017), which allows the comparison  
80 of the isoprenoid and branched GDGTs with other biomarkers and operationally-defined soil carbon pools.

### 2.2 Reference Materials for Method Validation

Evaluation of the isolation method involved assessment of the purity of separated fractions (i.e., potential interference from other than the desired compounds) and determination of the amount and isotopic composition external contamination introduced in course of the preparation sequence. For the latter, composites of different topsoil samples (0-5 cm) from a 30 x 30  
85 m grassland area in central Switzerland (5.9% C, bulk soil organic carbon (OC)  $F^{14}\text{C} = 1.155$ ) and a Rhineland lignite from



the early Miocene (Heumann and Litt, 2002)(62.3% OC, bulk  $F^{14}C = 0.003$ ) were used for assessment and validation with regard to contamination.

### 2.3 GDGT isolation for radiocarbon measurement

Despite the relative ease of detection of GDGTs using modern HPLC-mass spectrometry (MS) techniques, one challenge  
90 in the radiocarbon analysis of GDGTs in soil and sediment samples is their low abundance, with ambient concentrations of  
brGDGTs and isoGDGTs that are typically in the range of 10 to 1000 ng gdw<sup>-1</sup> and 1 to 100 ng gdw<sup>-1</sup> (grams dry weight)  
soil, respectively (Weijers et al., 2006b). A separation of individual GDGTs of the soil samples used in this study would  
require on average 3000 g of soil to reach the minimum recommended mass (~ 15 μg C) for high-precision compound-specific  
radiocarbon analysis (Haghipour et al., 2018). As extracting several kg of material is impractical, focused instead on pooled  
95 isolation and <sup>14</sup>C measurement of isoprenoid GDGTs and branched GDGTs, respectively, at the compound class level, due  
to the common putative biological precursors and biosynthetic formation pathways for each compound class (Schouten et al.,  
2013). For this study, the pooling of the GDGTs reduced the required initial sample size to a maximum of 500 gdw of soil. The  
extraction and purification of the compounds prior to HPLC analysis followed a procedure that is similar to that applied to samples processed for quantification of GDGTs (Freymond et al., 2017).

100 In brief:

lipids were extracted from dried soil samples using a microwave (CEM MARS 5) or an Energized Dispersive Guided Extraction  
(CEM EDGE) system. No difference in performance was observed for the different extraction systems. Samples were processed  
in batches of roughly 15 to 20 g of material. For microwave extraction the samples were transferred to the extraction vessels  
and covered by a dichloromethane (DCM):methanol (MeOH) 9:1 (v/v, 25 ml) solvent mixture. Extraction temperature was  
105 programmed to ramp to 100°C in 35 min and is subsequently held for 20 min. For EDGE extraction 25 ml DCM:MeOH 9:1  
(v/v) was used for extraction at 110°C for 2 min and subsequent rinsing with 15 ml followed by a second extraction with 5 ml  
of solvent at 100°C and rinsing with 35 ml. The process was repeated on additional sample batches to yield sufficient quantities  
of the target lipid compounds for <sup>14</sup>C analysis. Pooled extracts were then dried under nitrogen flow. After the addition of 5  
ml MilliQ water with NaCl the neutral phase was back-extracted with hexane (Hex) and separated on a 1% deactivated silica  
110 column into apolar and polar fractions with Hex:DCM 9:1 (v/v) and DCM:MeOH 1:1 (v/v) respectively. Polar fractions were  
dried under N<sub>2</sub>, then re-dissolved in Hex:2-propanol (IPA) 99:1 (v/v) and passed over 0.45 μm PTFE filters. A portion of  
the polar fraction was set aside (1%) and an internal C<sub>46</sub> GDGT standard (Huguet et al., 2006) was added to this aliquot to  
determine GDGT concentrations.

Polar fractions were separated on an Agilent 1260 HPLC-system coupled to an Agilent 1260 fraction collector. Separation was  
115 achieved on two Waters Aquity UHPLC HEB Hilic columns (1.7 μm, 2.1 x 150 mm) connected in series and preceded by a  
2.1 x 5 mm guard column (Hopmans et al., 2016). The columns were heated to 45°C and the flow rate set to 0.2 ml min<sup>-1</sup>. For  
the first 25 min, compounds elute isocratically with a solvent mixture of 18% Hex:IPA 9:1 (v/v) (solvent A) and 82% hexane  
(solvent B). For the next 15 min the proportion of solvent B was decreased linearly to 65% followed by a linear gradient  
to 0% solvent B in 20 min. The total runtime of one injection hence sums up to 60 min followed by 20 min reequilibration



120 with 82% solvent B. The fraction collection is solely based on retention times with the isoprenoid fraction being collected  
from 14.5 to 26 min and the branched fraction from 33 to 43 min (Figure 1). The retention time is recurrently monitored to  
avoid undetected drifts. The injection volume is set to 15  $\mu\text{l}$  corresponding to total GDGT amounts of 100 to 300  $\text{ng ml}^{-1}$ .  
Each sample was injected 10 times and fractions were pooled afterwards. The isolated compound classes and the subset of the  
initial polar fraction set aside previously were analyzed for purity and quantification using the same HPLC system coupled  
125 to a quadrupole mass spectrometer (Agilent 6130) according to Hopmans et al. (2016). The isolated fractions were dried and  
transferred into 0.025 ml tin capsules (Elementar 03951620). The capsules containing each sample were measured using an  
elemental analyzer coupled to a gas-ion-source equipped accelerator mass spectrometer (EA-AMS) (Haghipour et al., 2018) at  
the laboratory of Ion Beam Physics at ETH Zürich (Synal et al., 2007; Ruff et al., 2007). In all cases, sample sizes were  $> 15$   
 $\mu\text{g C}$ .

## 130 2.4 Soil turnover model

Turnover times of the individual compounds are calculated based on a steady state two-pool box model (e.g., Trumbore et al.,  
1996; Torn et al., 2009; Schrumpf and Kaiser, 2015; van der Voort et al., 2019). This model assumes two homogenous pools  
with a first-order decay rate, a fast-cycling and a passive pool. For each of the pools the  $F^{14}\text{C}$  is calculated independently  
(equation 1), where  $F^{14}\text{C}_{pool(t)}$  is the radiocarbon signal of the respective pool in the sampling year  $t$ ,  $\text{lag}$  is the number of  
135 years between  $\text{CO}_2$  fixation in plants and plant litter entering the soil,  $\lambda$  is the radioactive decay of  $^{14}\text{C}$  (1/8267 years), and  
 $k_{pool}$  is the decomposition rate constant.

$$F^{14}\text{C}_{pool(t)} = F^{14}\text{C}_{atm(t-lag)} * k_{pool} + F^{14}\text{C}_{pool(t-1)} * (1 - k_{pool} - \lambda) \quad (1)$$

The fraction-weighted sum of the  $F^{14}\text{C}$  of each of the pools is the modelled  $F^{14}\text{C}$  of the sample and depends on the  
decomposition rate constants of each pool  $k_1$  and  $k_2$ , as well as the relative size of the two pools. The  $\Delta^{14}\text{C}$  of atmospheric  
140  $\text{CO}_2$  was taken from Hua et al. (2013) from 1950 to 1986 and from Hammer and Levin (2017) for the years thereafter.

## 3 Results

### 3.1 Method Validation

Repetitive preparation of samples with 10 injections each reveals a recovery efficiency of  $0.85 \pm 0.05$ . Analysis of isolated  
fractions on a quadrupole mass spectrometer operated in scan mode (Agilent 6130) for all masses between  $m/z$  500 and 1500  
145 reveals that more than 95% of compounds in either fraction are comprised of masses assigned to GDGTs (Figure 1).



The extraneous contamination added in the preparatory process is assumed to be of constant mass  $m_c$  and radiocarbon signature  $F^{14}C_c$ . Therefore, the measured signal  $F^{14}C_m$  is a mixture of the sample and the contaminant according to equation 2:

$$F^{14}C_m = \frac{F^{14}C_s * m_s + F^{14}C_c * m_c}{m_s + m_c} \quad (2)$$

150  $F^{14}C_s$  and  $m_s$  are the true radiocarbon signal and carbon mass of the sample. The measured  $F^{14}C_m$  changes depending on the mass of the sample, as smaller masses are more strongly affected by the constant contamination. We assume that in samples with a bulk radiocarbon signal that is either completely modern or does not contain any  $^{14}C$  at all the compound-specific radiocarbon value is similar to the bulk. Therefore, a radiocarbon-modern sample, i.e., the topsoil composite, and the radiocarbon-dead lignite were prepared and measured repeatedly with different concentrations. The best fit for  $F^{14}C_c$  and  $m_c$   
155 to match the observed  $F^{14}C_m$  for both sets of measurements is calculated according to Haghypour et al. (2018).

The blank assessment (Figure 2) yields a contamination of  $2.62 \pm 0.79 \mu\text{g C}$  with a fraction modern of  $0.59 \pm 0.18$ , which is in range of previously determined contamination introduced by HPLC separation of lipids (e.g., Shah and Pearson, 2007; Birkholz et al., 2013). The impact of the constant contamination decreases as the sample mass increases. Therefore, the limit  
160 towards large carbon masses of the fitted curve is equivalent to the radiocarbon signal of the sample unaffected by extraneously introduced carbon. For both samples, this limit and hence the compound  $F^{14}C$  differs from the bulk  $F^{14}C$  of the initial material. In the topsoil reference the compounds are depleted in radiocarbon ( $F^{14}C = 0.94$ ) with respect to the source, in the lignite the GDGTs are enriched ( $F^{14}C = 0.06$ ).

The recommended sample size to reach a precision  $<5\%$  varies depending on the age of the sample. For samples with a  
165 radiocarbon age  $< 1800$  years ( $F^{14}C > 0.8$ ) a size of  $20 \mu\text{g C}$  is sufficient to reach the desired precision, while samples older than 6000 years ( $F^{14}C < 0.5$ ) require at least  $50 \mu\text{g C}$ . These uncertainties are taken into account when considering the GDGT  $^{14}C$  results for the soil samples measured in this study.

### 3.2 Vertical Distributions of GDGTs

In the pre-alpine soil from Beatenberg, concentrations of GDGTs are generally highest in the topsoil, where the isoprenoid  
170 and branched GDGTs are  $10$  and  $38 \mu\text{g gdw}^{-1}$  respectively, whereas corresponding concentrations in the top soil layer of the Lausanne soil are much lower,  $0.6$  and  $2 \mu\text{g gdw}^{-1}$ , respectively (Figure 3). The concentration of both groups of GDGTs decreases sharply with increasing soil depths, with approximately ten times the abundance of isoGDGTs and brGDGTs in the top 5 cm than a few centimeters below. In contrast, isoprenoid and branched GDGTs concentrations normalized to organic carbon (OC) content increase with depth in the Beatenberg soil from  $47 \mu\text{g gOC}^{-1}$  for isoGDGTs and from  $175 \mu\text{g gOC}^{-1}$  for  
175 brGDGTs in the top 5 cm to  $273 \mu\text{g gOC}^{-1}$  and  $80 \mu\text{g gOC}^{-1}$ , respectively, between 20 and 40 cm depth. In the Lausanne soil profile, the OC-normalized isoprenoid and branched concentrations drop from  $10 \mu\text{g gOC}^{-1}$  and  $39 \mu\text{g gOC}^{-1}$ , respectively, in the top 5 cm to  $4$  and  $13 \mu\text{g gOC}^{-1}$  between 10 and 20 cm depth, and then increase to  $14$  and  $12 \mu\text{g gOC}^{-1}$  between 60 and



80 cm.

The relative abundance of the individual brGDGTs also changes with soil depth, as reflected in the MBT'<sub>5Me</sub> and CBT' ratio  
180 (De Jonge et al., 2014). The MBT'<sub>5Me</sub> index does not exhibit significant variability in either soil profile, while the CBT' index  
increases with soil depth, especially in the Lausanne soil indicating a shift towards 6-methylated GDGTs (Figure 3).

### 3.3 Radiocarbon variations

The GDGT fractions prepared for AMS measurement contained between 30 and 80  $\mu\text{g C}$ , except for the brGDGTs in the 10  
to 20 cm depth interval in Beatenberg and the iso- and brGDGTs from 60 to 80 cm the Lausanne soil, which range between  
185 15 and 20  $\mu\text{g C}$ . The results of the radiocarbon measurements are shown in Figure 4, together with previously reported  $^{14}\text{C}$   
data for other soil carbon constituents (Van der Voort et al., 2017). In the Beatenberg profile, radiocarbon signatures of both  
isoprenoid and branched GDGTs closely follow the bulk OC with  $\Delta^{14}\text{C}$  values of -23 and -30 ‰, respectively, in the top 5 cm,  
and decreasing to -241 and -196 ‰ in the 20 to 40 cm depth interval, respectively. This contrasts with dissolved organic carbon  
(DOC), which exhibits  $^{14}\text{C}$ -enriched and relatively invariant  $\Delta^{14}\text{C}$  values throughout the soil profile (73 ‰ in the topsoil to  
190 24 ‰ in the deeper soil)(Figure 4). Overall,  $\Delta^{14}\text{C}$  values of both groups of GDGTs are similar to those of a C<sub>29</sub> n-alkane and  
the long-chained (>C<sub>26</sub>) n-alkanoic fatty acids (FA), but differ sharply from those of shorter-chained (C<sub>16</sub>-C<sub>22</sub> measured on  
the same samples (Van der Voort et al., 2017). The latter never reach  $\Delta^{14}\text{C}$  values lower than -90 ‰ in the soils, resulting in  
an offset between short-chained fatty acids and the other analyzed compounds that show stronger decreases with soil depth.  
Similar patterns exist in the Lausanne profile: The  $\Delta^{14}\text{C}$  values in isoprenoid and branched GDGTs decrease with depth from  
195 -20 and -7 ‰ at 0 to 5 cm to -441 and -310 ‰ at 60 to 80 cm, respectively. While  $\Delta^{14}\text{C}$  values of bulk OC and GDGTs parallel  
one another closely in the Beatenberg soil, GDGT  $\Delta^{14}\text{C}$  values are systematically lower than bulk OC and at each depth  
interval in the Lausanne profile, with the difference between GDGTs and bulk OC ranging from -105 to -200 ‰. The GDGT  
 $\Delta^{14}\text{C}$  values are also more depleted than those of DOC and short-chain (C<sub>16-22</sub>) FA in the soil, but are bracketed by n-C<sub>27</sub> n-  
alkane and n-C<sub>29</sub> fatty acid  $\Delta^{14}\text{C}$  values in the deepest soil section (Van der Voort et al., 2017). The  $\Delta^{14}\text{C}$  values of the density  
200 fractions from the same soil samples were also measured by Van der Voort et al. (2017). The low density fraction corresponds  
to the free particulate organic carbon (free POC) and the high density fraction is interpreted as mineral-associated POC. Both  
fractions do not differ by more than 40 ‰ in the top 20 cm of either soil profile, but in the lowest depth interval the fractions  
diverge, with markedly lower  $\Delta^{14}\text{C}$  values the for high density fraction, and values similar to DOC for the free POC fraction.  
In both soils, the iso and brGDGTs exhibit similar or lower  $\Delta^{14}\text{C}$  values than the high density fraction, mineral-associated  
205 organic matter fraction.

### 3.4 Radiocarbon derived turnover times of GDGTs

Turnover times of the compounds are calculated based on a two-pool model that requires three parameters to be fitted: the  
turnover time of the fast-cycling pool, the turnover time of the passive pool and the proportion of the fast-cycling pool. As only  
one radiocarbon measurement per compound and depth interval is available, two of the parameters need to be estimated, while  
210 one can be fitted accordingly. We use the proportion of the labile low-density fraction of the samples (Van der Voort et al.,



2017) to constrain the size of the fast-cycling pool. The turnover time of the fast-cycling pool can be estimated accordingly as the single-pool turnover time of the light fraction. Alternatively, the GDGT turnover in topsoil based on stable carbon isotopes has been shown to be similar to short-chain fatty acids (Weijers et al., 2010; Huguet et al., 2017). Thus, the turnover time of these compounds based on a single-pool box model can also be used to constrain turnover time of the fast-cycling pool of GDGTs. For simplicity, a lag-term addressing the time between atmospheric carbon fixation and input into the soil is not used, as it is shorter than a decade (Solly et al., 2018) and its potential influence is hence already covered by the range of the turnover time estimates of the fast pool. The low  $\Delta^{14}\text{C}$  values of GDGTs in the deeper soil intervals result in a turnover time of the passive GDGT pool in the order of 1400 to 2000 years between 10 and 20 cm depth and 2000 up to 6000 years in the lowest depth interval in either soil (Table 1). These results are insensitive to changes of either the turnover time and the size of the labile pool: A change of  $\pm 10\%$  of the proportion of the fast pool or  $\pm 500$  years of the turnover time of the fast pool results in a maximum change of  $10\%$  of the overall GDGT turnover time in the two lower depth intervals in either soil. Thus, despite the uncertainties in the estimation of the proportion of the pools and the turnover time of the fast pool, the turnover time of both groups of GDGTs clearly exceeds a millenium.

## 4 Discussion

### 4.1 Efficacy of GDGT isolation and $^{14}\text{C}$ measurement protocol

Compared to prior methods to achieve individual isoGDGT separation by HPLC (Smittenberg et al., 2002; Ingalls et al., 2006), the introduced method isolates GDGTs only at the compound-class level, hence potential radiocarbon variations among GDGT isomers are not discernable. However, previous analyses of stable carbon isotopic as well as radiocarbon analysis of GDGTs on a molecular level do not show significant differences between the individual isoprenoid or branched GDGTs, respectively (e.g., Ingalls et al., 2006; Shah et al., 2008; Oppermann et al., 2010; Weber et al., 2015). This implies similar metabolisms for brGDGT-producing organisms and also for microbial communities that synthesize isoGDGTs. Consequently, pooling of isomers within a compound class according to their respective microbial domain (bacteria, archaea) seems reasonable, particularly given the practical constraints imposed by their low abundance in many terrestrial (and aquatic) environments. The introduced method requires only a single normal-phase isolation step using the same columns that are used for quantification of GDGTs (Hopmans et al., 2016), minimizing the time required for sample preparation and without extensive adjustments to the analytical HPLC set-up. The calculated contamination is in range of the blank assessment by Ingalls et al. (2006), but higher than the extraneous carbon observed by Birkholz et al. (2013). However, the blank assessment in Birkholz et al. (2013) is based only on a modern non-GDGT standard (cholesterol), potentially leading to an underestimation of the sample preparation blank.

The GDGT-specific  $\Delta^{14}\text{C}$  values of the top soil and lignite samples used as "modern" and "fossil" endmembers for blank assessment did not yield values that fully matched those expected given their age. In case of the soil, different  $\Delta^{14}\text{C}$  values of the GDGTs compared to bulk OC are to be expected due to the heterogeneous nature of soil organic matter, however for lignite sample that is of geologic age ( $> 30$  Ma), all components would be expected to be radiocarbon-dead. A preliminary batch of



lignite that was extracted yielded 18  $\mu\text{g C}$  of isoGDGTs and 48  $\mu\text{g C}$  of brGDGTs, with corresponding  $\Delta^{14}\text{C}$  values of the  
245 resulting isolated compounds of -960‰ and -980‰, respectively. The second batch of lignite used to assess constant con-  
tamination was prepared 4 months later and shows  $\Delta^{14}\text{C}$  values consistently higher than -950‰ (figure 2). This shift towards  
higher  $\Delta^{14}\text{C}$  values likely reflects contamination resulting from sample-to-sample carry-over on the HPLC. Although this is  
addressed in the blank assessment, this highlights the importance of repeated blank assessment in order to control for variations  
in carry-over and other potential sources of contamination (e.g., column bleed) over time. Careful assessment of compound  
250 purity is also important to ensure robust isotopic determination.

#### 4.2 Radiocarbon constraints on the origin and turnover of GDGTs in soils

Our study reveals low  $\Delta^{14}\text{C}$  values, with corresponding radiocarbon ages of up to 6000 years for GDGTs in forested soils.  
These  $^{14}\text{C}$  characteristics are similar to those of the mineral-associated OM (from density fractionation), as well as long-chain,  
higher plant wax-derived n-fatty acids and n-alkanes. As GDGTs are microbial membrane lipids, these findings reveal the  
255 presence of  $^{14}\text{C}$ -depleted, millennial age microbial residues as a component of organic matter in deeper soils. There are two  
possible pathways leading to these old apparent radiocarbon ages: (1) active GDGT-producing heterotrophic soil microbial  
communities in deeper soils are utilizing pre-aged SOM as a carbon source, and accrue this signal with continuous community  
turnover. Alternatively, (2) upon cell death these microbial lipids are stabilized for millenia, likely via interaction with soil  
minerals. We first consider the first explanation:

260 The  $\Delta^{14}\text{C}$  values of living organisms, and their constituent lipids, directly reflect that of their metabolic carbon source  
as, unlike stable isotopes, they are impervious to biological fractionation effects (Ingalls and Pearson, 2005). Upon death  
of the organism, radioactive decay leads to depletion in  $^{14}\text{C}$  contents. Consequently, the  $^{14}\text{C}$  contents of iso- and brGDGTs  
should reflect that of the carbon source of their biological precursors. IsoGDGTs are known to be produced by Thaumarcheota  
and Euryarcheota (Schouten et al., 2013). The specific microbes that produce brGDGTs are yet to be identified, there is  
265 strong evidence that the precursor organisms are heterotrophic bacteria (Pancost and Damsté, 2003; Weijers et al., 2010),  
with Acidobacteria amongst the candidate phyla (Damsté et al., 2018). For heterotrophic bacteria, potential carbon sources  
include DOC leached from the organic layer, exudates from root systems or organic matter that has accumulated during soil  
development. The activity of soil microbial communities has often been assayed using phospholipid-fatty acids (PLFAs), as  
phospholipids are only found in living cells and thus serve as biomarkers for viable microbial communities (e.g., Tunlid and  
270 White, 1991). Compound-specific radiocarbon analyses of PLFAs have shown that soil microbes can use a variety of carbon  
sources, including “older” SOM (Kramer and Gleixner, 2006). However, root-derived C seems a dominant food source of  
heterotrophic microbial communities in temperate deciduous forest soils (Kramer et al., 2010) and this has been inferred to  
be a likely substrate for the producers of brGDGTs (Huguet et al., 2013). The turnover time of root carbon is on the order  
of decades at most (Gill and Jackson, 2000; Gaudinski et al., 2001; Solly et al., 2018)), and thus the old ages and long  
275 turnover times of GDGTs observed in both soils analyzed in this study cannot be explained by the uptake of root-derived C.  
Accessible, labile carbon pools in the investigated soil profiles are represented by DOC and the light density fraction. These  
appear to be preferably used by microbial communities as evidenced by the  $^{14}\text{C}$ -enriched values of short-chain ( $<\text{C}_{24}$ ) fatty



acids that likely reflect active microbial communities (Figure 4, 5). The markedly lower  $\Delta^{14}C$  values of both isoGDGTs and brGDGTs at depth would require that both groups of precursor organisms, i.e., Archaea and Bacteria, occupy specific niches using metabolic strategies that enable them to utilize stabilized, aged carbon. The precursor organisms of isoGDGTs in soils are known to be mainly comprised of crenarchaeota, i.e., chemoautotrophic nitrifiers using soil  $CO_2$  as substrate (Leininger et al., 2006; Urich et al., 2008; Weijers et al., 2010; Damsté et al., 2012) and acetotrophic methanogens (Weijers et al., 2010). Contributions from the latter organisms in the studied soils are likely minor as the soils are not strictly anaerobic (Walthert, 2003)). This is also supported by GDGT-0/Crenarchaeol ratios, that differ sharply from those in soils and sediments dominated by methanogens (Blaga et al., 2009; Weijers et al., 2010; Naeher et al., 2014). Soil-respired  $CO_2$  has relatively high  $\Delta^{14}C$  values (Gaudinski et al., 2000; Liu et al., 2006), and thus it seems highly unlikely that  $^{14}C$ -depleted signatures of isoGDGTs in the deeper soils results from metabolism of an old C substrate by active soil microbial communities. By analogy, the  $^{14}C$ -depleted characteristics of brGDGTs is difficult to reconcile with heterotrophic consumption of pre-aged C. Overall, the contrasting metabolisms of the GDGT precursor organisms (primarily autotrophy for isoGDGTs and heterotrophy for brGDGTs), yet similar (and low)  $\Delta^{14}C$  values for both compound classes, argue against an origin of the GDGT signals from microbial growth at depth. We therefore conclude that uptake of pre-aged carbon by active soil microbial communities is unlikely to be the cause for the  $^{14}C$ -depleted GDGT signatures.

We next consider the long-term stabilization microbially-derived carbon as the source of  $^{14}C$ -depleted GDGT signatures. This implies that microbial residues persist in soils for millennia, lending support to emerging concepts that microbial necromass comprises an important component of older SOM (e.g., Lehmann and Kleber, 2015; Liang et al., 2017). Long-term persistence of GDGTs could arise from their stabilization by soil minerals at greater soil depths. The amphiphilic nature of lipids such as GDGTs, with both polar and hydrophobic components, promotes the association with mineral surfaces, and therefore may afford physical protection from degradation (Jandl et al., 2004; Kleber et al., 2007; von Lützow et al., 2008; Van der Voort et al., 2017). By comparison, in surface soils with high organic matter contents and less availability of reactive mineral surfaces, GDGTs are continuously produced and degraded, which results in a younger mean radiocarbon age and evidence for turnover on decadal timescales (Weijers et al., 2010). This explanation agrees with conceptual models of soil organic matter dynamics whereby older SOM in deeper soils primarily consists of microbial metabolites that are stabilized by their interaction with mineral surfaces (Schmidt et al., 2011; Lehmann and Kleber, 2015). Given the structural resemblance between brGDGTs and isoGDGTs, and hence similar propensity to associate with mineral surfaces, we consider this a more likely explanation for their similarly old  $^{14}C$  ages than “niche metabolisms” of different precursor organisms. The older GDGT age in the Cambisol at Lausanne compared to the subalpine Podzol at Beatenberg with a bleached eluvial horizon also supports this conclusion. The higher contents of clay and highly reactive amorphous Fe and Al-oxides and hydroxides of the former (Table 2) are known to play a key role in the sorptive stabilization of SOM (Kaiser and Guggenberger, 2003; Kleber et al., 2007)

Overall,  $^{14}C$  characteristics of iso and brGDGTs and the inferred turnover times that are far longer than those of discrete POM (free light density fraction) and signature lipids of active microbial communities (short-chained fatty acids), but similar to those



of plant-derived long-chain n-alkanes and fatty acids (Figure 5), serve as strong evidence for the presence of mineral-stabilized microbial necromass in the studied forested mineral soils.

### 4.3 Implications for application of GDGTs as molecular proxies and soil tracer biomolecules

315 In addition to the insights into soil carbon turnover, the observed  $^{14}\text{C}$  signatures of GDGTs in the two soil profiles carry impli-  
cations for their application as proxies of environmental conditions and as tracers of soil carbon input to aquatic environments.  
Several studies have shown that soils comprise a significant, and often the dominant, component of terrestrial organic carbon  
exported in the suspended load of rivers to lake and ocean sediments (e.g., Tao et al., 2015; Vonk et al., 2019; Hein et al., 2020).  
Prior analyses of branched GDGTs in sedimentary archives have revealed older GDGT ages than depositional ages (Smitten-  
320 berg et al., 2005; Birkholz et al., 2013) that may reflect intermittent storage during transport or export of deeper mineral soil  
carbon suggesting a lag between production and deposition. Our findings suggest that this may be a consequence of protracted  
storage in and mobilization from deeper mineral soils. This reinforces the value of brGDGTs as tracers of soil carbon, but  
implies that much of the signal may be sourced from deeper soil layers, with corresponding GDGT proxy signals reflecting  
environmental conditions at the time that they were microbially produced.

## 325 5 Conclusions

We modified and validated a normal-phase HPLC method to isolate isoprenoid and branched GDGTs at the compound class  
level for radiocarbon analysis. Although further refinements in the method would be desirable, this new approach yields reliable  
GDGT  $^{14}\text{C}$  measurements on sample sizes  $> 20 \mu\text{g C}$  that have enabled novel questions to be addressed concerning the  
provenance and turnover of this key suite of microbial lipids. In addition to its application to questions of soil C cycling, the  
330 streamlined method opens up new opportunities to further explore the biogeochemical and paleoclimate significance of this  
intriguing yet enigmatic class of lipids.

Application of the method to depth profiles for two well-studied sub-alpine soil profiles in Switzerland reveals a marked  
decrease in  $^{14}\text{C}$  contents of both isoGDGTs and brGDGTs with depth, with resulting model estimates for GDGT turnover  
times of 2000 to 6000 years in deeper mineral soils. These old ages for archaeal and bacterial membrane lipids provides  
335 compelling evidence for stabilization of microbial necromass in soils that contributes to the long-term C storage. Through  
comparison with parallel  $^{14}\text{C}$  data for soil density fractions and other hydrophobic lipid biomarkers, we attribute the stability  
of GDGTs to protection via association with reactive mineral surfaces underlining the crucial role of microbial processes in  
soil C cycling and stabilization.

Our findings also provide motivation for further work to validate our interpretations and assess the broader significance of the  
340 current limited suite of observations. For example, comparison of the proportions and isotopic signatures of intact polar lipid  
GDGTs relative to the “core” lipids measured here could shed light on the significance active GDGT-producing communities  
residing at a specific soil depth versus remnants of past microbial activity (necromass). Furthermore, while concentrations of  
isoprenoid as well as branched GDGTs commonly decrease with increasing soil depth (Huguet et al., 2010; Yamamoto et al.,



2016; Gocke et al., 2017), subsurface maxima in iso- and brGDGT concentrations have also been reported (Huguet et al.,  
345 2010; Yamamoto et al., 2016)), potentially indicating depth-localized GDGT production. Future  $^{14}\text{C}$  analysis of GDGTs in  
soil profiles that exhibit such sub-surface concentrations peak would be informative and provide context for our observations  
in the two Swiss soil profiles. Further insights into the provenance and turnover of brGDGTs might be gained from in-depth  
assessment of molecular distributions and associated proxy indices (De Jonge et al., 2014), that may reflect changes in current  
or past microbial communities, or imply differences in susceptibility to degradation. Despite the presence of GDGTs as trace  
350 constituents of SOM, their unequivocal microbial origin, distinctive chemical structures, and environmental properties that  
their distributions encode render them powerful tracer compounds and molecular proxies. Here, we demonstrate that when  
also constrained with natural abundance  $^{14}\text{C}$ , these compounds provide a new window into the role of microorganisms in soil  
carbon cycling.

*Code and data availability.* The data set and script for the turnover model used in this study is available at [https://doi.org/10.3929/ethz-b-](https://doi.org/10.3929/ethz-b-000430425)  
355 000430425

*Author contributions.* HG, ML and TE conceptualized the study, HG and DM designed the method, HG isolated the compounds and wrote  
the turnover model, NH performed radiocarbon measurements, TSvdV provided data, HG, FH, ML and TE interpreted the data, HG prepared  
the manuscript with contributions from all co-authors.

*Competing interests.* The authors declare that they have no competing interests

360 *Acknowledgements.* This study was funded by the Swiss National Science Foundation (“CAPS-LOCK2” & “CAPS-LOCK3”; #184865). We  
thank Urs Overhoff and Markus Neuroth from the RWE Power AG for the provisioning of the lignite sample, and Marco Griepentrog  
and Cindy de Jonge for helpful discussions. We thank the Laboratory for Ion Beam Physics (ETH) for support with the Accelerator Mass  
Spectrometry measurements.



## References

- 365 Ahrens, B., Braakhekke, M. C., Guggenberger, G., Schrumpp, M., and Reichstein, M.: Contribution of sorption, DOC transport and microbial interactions to the  $^{14}\text{C}$  age of a soil organic carbon profile: Insights from a calibrated process model, *Soil Biology and Biochemistry*, 88, 390–402, 2015.
- Amelung, W., Brodowski, S., Sandhage-Hofmann, A., and Bol, R.: Combining biomarker with stable isotope analyses for assessing the transformation and turnover of soil organic matter, *Advances in agronomy*, 100, 155–250, 2008.
- 370 Battin, T. J., Luysaert, S., Kaplan, L. A., Aufdenkampe, A. K., Richter, A., and Tranvik, L. J.: The boundless carbon cycle, *Nature Geoscience*, 2, 598–600, 2009.
- Birkholz, A., Smittenberg, R. H., Hajdas, I., Wacker, L., and Bernasconi, S. M.: Isolation and compound specific radiocarbon dating of terrigenous branched glycerol dialkyl glycerol tetraethers (brGDGTs), *Organic geochemistry*, 60, 9–19, 2013.
- Blaga, C. I., Reichart, G.-J., Heiri, O., and Damsté, J. S. S.: Tetraether membrane lipid distributions in water-column particulate matter and  
375 sediments: a study of 47 European lakes along a north–south transect, *Journal of Paleolimnology*, 41, 523–540, 2009.
- Bradford, M. A., Wieder, W. R., Bonan, G. B., Fierer, N., Raymond, P. A., and Crowther, T. W.: Managing uncertainty in soil carbon feedbacks to climate change, *Nature Climate Change*, 6, 751–758, 2016.
- Carvalhais, N., Forkel, M., Khomik, M., Bellarby, J., Jung, M., Migliavacca, M., Saatchi, S., Santoro, M., Thurner, M., Weber, U., et al.: Global covariation of carbon turnover times with climate in terrestrial ecosystems, *Nature*, 514, 213–217, 2014.
- 380 Coffinet, S., Hugué, A., Williamson, D., Fosse, C., and Derenne, S.: Potential of GDGTs as a temperature proxy along an altitudinal transect at Mount Rungwe (Tanzania), *Organic geochemistry*, 68, 82–89, 2014.
- Cotrufo, M. F., Soong, J. L., Horton, A. J., Campbell, E. E., Haddix, M. L., Wall, D. H., and Parton, W. J.: Formation of soil organic matter via biochemical and physical pathways of litter mass loss, *Nature Geoscience*, 8, 776–779, 2015.
- Damsté, J. S. S., Rijpstra, W. I. C., Hopmans, E. C., Jung, M.-Y., Kim, J.-G., Rhee, S.-K., Stieglmeier, M., and Schleper, C.: Intact polar  
385 and core glycerol dibiphytanyl glycerol tetraether lipids of group I. 1a and I. 1b Thaumarchaeota in soil, *Appl. Environ. Microbiol.*, 78, 6866–6874, 2012.
- Damsté, J. S. S., Rijpstra, W. I. C., Foesel, B. U., Huber, K. J., Overmann, J., Nakagawa, S., Kim, J. J., Dunfield, P. F., Dedysh, S. N., and Villanueva, L.: An overview of the occurrence of ether- and ester-linked iso-diabolic acid membrane lipids in microbial cultures of the *Acidobacteria*: Implications for brGDGT paleoproxies for temperature and pH, *Organic Geochemistry*, 124, 63–76, 2018.
- 390 De Jonge, C., Hopmans, E. C., Zell, C. I., Kim, J.-H., Schouten, S., and Damsté, J. S. S.: Occurrence and abundance of 6-methyl branched glycerol dialkyl glycerol tetraethers in soils: Implications for palaeoclimate reconstruction, *Geochimica et Cosmochimica Acta*, 141, 97–112, 2014.
- De Rosa, M. and Gambacorta, A.: The lipids of archaeobacteria, *Progress in lipid research*, 27, 153–175, 1988.
- Freymond, C. V., Peterse, F., Fischer, L. V., Filip, F., Giosan, L., and Eglinton, T. I.: Branched GDGT signals in fluvial sediments of the  
395 Danube River basin: Method comparison and longitudinal evolution, *Organic geochemistry*, 103, 88–96, 2017.
- Gaudinski, J., Trumbore, S., Davidson, E., Cook, A., Markewitz, D., and Richter, D.: The age of fine-root carbon in three forests of the eastern United States measured by radiocarbon, *Oecologia*, 129, 420–429, 2001.
- Gaudinski, J. B., Trumbore, S. E., Davidson, E. A., and Zheng, S.: Soil carbon cycling in a temperate forest: radiocarbon-based estimates of residence times, sequestration rates and partitioning of fluxes, *Biogeochemistry*, 51, 33–69, 2000.
- 400 Gill, R. A. and Jackson, R. B.: Global patterns of root turnover for terrestrial ecosystems, *The New Phytologist*, 147, 13–31, 2000.



- Gleixner, G.: Soil organic matter dynamics: a biological perspective derived from the use of compound-specific isotopes studies, *Ecological research*, 28, 683–695, 2013.
- Gocke, M. I., Huguet, A., Derenne, S., Kolb, S., Dippold, M. A., and Wiesenberg, G. L.: Disentangling interactions between microbial communities and roots in deep subsoil, *Science of the Total Environment*, 575, 135–145, 2017.
- 405 Haghypour, N., Ausin, B., Usman, M. O., Ishikawa, N., Wacker, L., Welte, C., Ueda, K., and Eglinton, T. I.: Compound-Specific Radiocarbon Analysis by Elemental Analyzer–Accelerator Mass Spectrometry: Precision and Limitations, *Analytical chemistry*, 91, 2042–2049, 2018.
- Hammer, S. and Levin, I.: Monthly mean atmospheric  $\Delta^{14}\text{CO}_2$  at Jungfraujoch and Schauinsland from 1986 to 2016, *heiDATA*, 2, 2017.
- He, N. and Yu, G.: Stoichiometrical regulation of soil organic matter decomposition and its temperature sensitivity, *Ecology and evolution*, 6, 620–627, 2016.
- 410 Hein, C. J., Usman, M., Eglinton, T. I., Haghypour, N., and Galy, V. V.: Millennial-scale hydroclimate control of tropical soil carbon storage, *Nature*, 581, 63–66, 2020.
- Heumann, G. and Litt, T.: Stratigraphy and paleoecology of the Late Pliocene and Early Pleistocene in the open-cast mine Hambach (Lower Rhine Basin), *Netherlands Journal of Geosciences*, 81, 193–199, 2002.
- Hopmans, E. C., Weijers, J. W., Schefuß, E., Herfort, L., Damsté, J. S. S., and Schouten, S.: A novel proxy for terrestrial organic matter in  
415 sediments based on branched and isoprenoid tetraether lipids, *Earth and Planetary Science Letters*, 224, 107–116, 2004.
- Hopmans, E. C., Schouten, S., and Damsté, J. S. S.: The effect of improved chromatography on GDGT-based palaeoproxies, *Organic Geochemistry*, 93, 1–6, 2016.
- Hua, Q., Barbetti, M., and Rakowski, A. Z.: Atmospheric radiocarbon for the period 1950–2010, *Radiocarbon*, 55, 2059–2072, 2013.
- Huang, Y., Li, B., Bryant, C., Bol, R., and Eglinton, G.: Radiocarbon dating of aliphatic hydrocarbons a new approach for dating passive-  
420 fraction carbon in soil horizons, *Soil Science Society of America Journal*, 63, 1181–1187, 1999.
- Huguet, A., Fosse, C., Metzger, P., Fritsch, E., and Derenne, S.: Occurrence and distribution of non-extractable glycerol dialkyl glycerol tetraethers in temperate and tropical podzol profiles, *Organic Geochemistry*, 41, 833–844, 2010.
- Huguet, A., Gocke, M., Derenne, S., Fosse, C., and Wiesenberg, G. L.: Root-associated branched tetraether source microorganisms may reduce estimated paleotemperatures in subsoil, *Chemical Geology*, 356, 1–10, 2013.
- 425 Huguet, A., Meador, T. B., Laggoun-Défarge, F., Könneke, M., Wu, W., Derenne, S., and Hinrichs, K.-U.: Production rates of bacterial tetraether lipids and fatty acids in peatland under varying oxygen concentrations, *Geochimica et Cosmochimica Acta*, 203, 103–116, 2017.
- Huguet, C., Hopmans, E. C., Febo-Ayala, W., Thompson, D. H., Damsté, J. S. S., and Schouten, S.: An improved method to determine the absolute abundance of glycerol dibiphytanyl glycerol tetraether lipids, *Organic Geochemistry*, 37, 1036–1041, 2006.
- 430 Ingalls, A. E. and Pearson, A.: Compound-Specific Radiocarbon Analysis, *Oceanography*, 18, 18–31, 2005.
- Ingalls, A. E., Shah, S. R., Hansman, R. L., Aluwihare, L. I., Santos, G. M., Druffel, E. R., and Pearson, A.: Quantifying archaeal community autotrophy in the mesopelagic ocean using natural radiocarbon, *Proceedings of the National Academy of Sciences*, 103, 6442–6447, 2006.
- Innes, J. L.: Theoretical and practical criteria for the selection of ecosystem monitoring plots in Swiss forests, *Environmental Monitoring and Assessment*, 36, 271–294, 1995.
- 435 Jandl, G., Leinweber, P., Schulten, H.-R., and Eusterhues, K.: The concentrations of fatty acids in organo-mineral particle-size fractions of a Chernozem, *European Journal of Soil Science*, 55, 459–470, 2004.
- Kaiser, K. and Guggenberger, G.: Mineral surfaces and soil organic matter, *European Journal of Soil Science*, 54, 219–236, 2003.



- Kallenbach, C. M., Frey, S. D., and Grandy, A. S.: Direct evidence for microbial-derived soil organic matter formation and its ecophysiological controls, *Nature communications*, 7, 13 630, 2016.
- 440 Kästner, M. and Miltner, A.: SOM and microbes—What is left from microbial life, in: *The future of soil carbon*, pp. 125–163, Elsevier, 2018.
- Kleber, M., Sollins, P., and Sutton, R.: A conceptual model of organo-mineral interactions in soils: self-assembly of organic molecular fragments into zonal structures on mineral surfaces, *Biogeochemistry*, 85, 9–24, 2007.
- Kramer, C. and Gleixner, G.: Variable use of plant- and soil-derived carbon by microorganisms in agricultural soils, *Soil Biology and Biochemistry*, 38, 3267–3278, 2006.
- 445 Kramer, C. and Gleixner, G.: Soil organic matter in soil depth profiles: distinct carbon preferences of microbial groups during carbon transformation, *Soil Biology and Biochemistry*, 40, 425–433, 2008.
- Kramer, C., Trumbore, S., Fröberg, M., Dozal, L. M. C., Zhang, D., Xu, X., Santos, G. M., and Hanson, P. J.: Recent (< 4 year old) leaf litter is not a major source of microbial carbon in a temperate forest mineral soil, *Soil Biology and Biochemistry*, 42, 1028–1037, 2010.
- Lehmann, J. and Kleber, M.: The contentious nature of soil organic matter, *Nature*, 528, 60–68, 2015.
- 450 Leininger, S., Urich, T., Schloter, M., Schwark, L., Qi, J., Nicol, G. W., Prosser, J. I., Schuster, S., and Schleper, C.: Archaea predominate among ammonia-oxidizing prokaryotes in soils, *Nature*, 442, 806–809, 2006.
- Liang, C., Schimel, J. P., and Jastrow, J. D.: The importance of anabolism in microbial control over soil carbon storage, *Nature microbiology*, 2, 1–6, 2017.
- Liang, C., Amelung, W., Lehmann, J., and Kästner, M.: Quantitative assessment of microbial necromass contribution to soil organic matter, *Global change biology*, 25, 3578–3590, 2019.
- 455 Liu, W., Moriizumi, J., Yamazawa, H., and Iida, T.: Depth profiles of radiocarbon and carbon isotopic compositions of organic matter and CO<sub>2</sub> in a forest soil, *Journal of environmental radioactivity*, 90, 210–223, 2006.
- Liu, W., Wang, H., Zhang, C. L., Liu, Z., and He, Y.: Distribution of glycerol dialkyl glycerol tetraether lipids along an altitudinal transect on Mt. Xiangpi, NE Qinghai-Tibetan Plateau, China, *Organic Geochemistry*, 57, 76–83, 2013.
- 460 Ma, T., Zhu, S., Wang, Z., Chen, D., Dai, G., Feng, B., Su, X., Hu, H., Li, K., Han, W., et al.: Divergent accumulation of microbial necromass and plant lignin components in grassland soils, *Nature communications*, 9, 1–9, 2018.
- Matsumoto, K., Kawamura, K., Uchida, M., and Shibata, Y.: Radiocarbon content and stable carbon isotopic ratios of individual fatty acids in subsurface soil: Implication for selective microbial degradation and modification of soil organic matter, *Geochemical Journal*, 41, 483–492, 2007.
- 465 Miltner, A., Bombach, P., Schmidt-Brücken, B., and Kästner, M.: SOM genesis: microbial biomass as a significant source, *Biogeochemistry*, 111, 41–55, 2012.
- Mollenhauer, G., Inthorn, M., Vogt, T., Zabel, M., Sinnighe Damsté, J. S., and Eglinton, T. I.: Aging of marine organic matter during cross-shelf lateral transport in the Benguela upwelling system revealed by compound-specific radiocarbon dating, *Geochemistry, Geophysics, Geosystems*, 8, 2007.
- 470 Mollenhauer, G., Eglinton, T. I., Hopmans, E. C., and Damsté, J. S. S.: A radiocarbon-based assessment of the preservation characteristics of crenarchaeol and alkenones from continental margin sediments, *Organic Geochemistry*, 39, 1039–1045, 2008.
- Naafs, B., Gallego-Sala, A., Inglis, G., and Pancost, R.: Refining the global branched glycerol dialkyl glycerol tetraether (brGDGT) soil temperature calibration, *Organic Geochemistry*, 106, 48–56, 2017.



- 475 Naeher, S., Peterse, F., Smittenberg, R. H., Niemann, H., Zigah, P. K., and Schubert, C. J.: Sources of glycerol dialkyl glycerol tetraethers (GDGTs) in catchment soils, water column and sediments of Lake Rotsee (Switzerland)—Implications for the application of GDGT-based proxies for lakes, *Organic geochemistry*, 66, 164–173, 2014.
- Oppermann, B., Michaelis, W., Blumenberg, M., Frerichs, J., Schulz, H.-M., Schippers, A., Beaubien, S., and Krüger, M.: Soil microbial community changes as a result of long-term exposure to a natural CO<sub>2</sub> vent, *Geochimica et Cosmochimica Acta*, 74, 2697–2716, 2010.
- 480 Pancost, R. D. and Damsté, J. S. S.: Carbon isotopic compositions of prokaryotic lipids as tracers of carbon cycling in diverse settings, *Chemical Geology*, 195, 29–58, 2003.
- Parry, M., Parry, M. L., Canziani, O., Palutikof, J., Van der Linden, P., Hanson, C., et al.: *Climate change 2007-impacts, adaptation and vulnerability: Working group II contribution to the fourth assessment report of the IPCC*, vol. 4, Cambridge University Press, 2007.
- Pearson, A., McNichol, A. P., Benitez-Nelson, B. C., Hayes, J. M., and Eglinton, T. I.: Origins of lipid biomarkers in Santa Monica Basin surface sediment: a case study using compound-specific  $\Delta^{14}\text{C}$  analysis, *Geochimica et Cosmochimica Acta*, 65, 3123–3137, 2001.
- 485 Peterse, F., van der Meer, J., Schouten, S., Weijers, J. W., Fierer, N., Jackson, R. B., Kim, J.-H., and Damsté, J. S. S.: Revised calibration of the MBT–CBT paleotemperature proxy based on branched tetraether membrane lipids in surface soils, *Geochimica et Cosmochimica Acta*, 96, 215–229, 2012.
- Powers, L., Werne, J. P., Vanderwoude, A. J., Damsté, J. S. S., Hopmans, E. C., and Schouten, S.: Applicability and calibration of the TEX<sub>86</sub> paleothermometer in lakes, *Organic Geochemistry*, 41, 404–413, 2010.
- 490 Powers, L. A., Werne, J. P., Johnson, T. C., Hopmans, E. C., Damsté, J. S. S., and Schouten, S.: Crenarchaeotal membrane lipids in lake sediments: a new paleotemperature proxy for continental paleoclimate reconstruction?, *Geology*, 32, 613–616, 2004.
- Riley, W., Maggi, F., Kleber, M., Torn, M., Tang, J., Dwivedi, D., and Guerry, N.: Long residence times of rapidly decomposable soil organic matter: application of a multi-phase, multi-component, and vertically resolved model (BAMS1) to soil carbon dynamics, *Geoscientific Model Development*, 7, 2014.
- 495 Ruff, M., Wacker, L., Gäggeler, H., Suter, M., Synal, H.-A., and Szidat, S.: A gas ion source for radiocarbon measurements at 200 kV, *Radiocarbon*, 49, 307–314, 2007.
- Schmidt, M. W., Torn, M. S., Abiven, S., Dittmar, T., Guggenberger, G., Janssens, I. A., Kleber, M., Kögel-Knabner, I., Lehmann, J., Manning, D. A., et al.: Persistence of soil organic matter as an ecosystem property, *Nature*, 478, 49–56, 2011.
- Schouten, S., Hopmans, E. C., Schefuß, E., and Damsté, J. S. S.: Distributional variations in marine crenarchaeotal membrane lipids: a new 500 tool for reconstructing ancient sea water temperatures?, *Earth and Planetary Science Letters*, 204, 265–274, 2002.
- Schouten, S., Hopmans, E. C., and Damsté, J. S. S.: The organic geochemistry of glycerol dialkyl glycerol tetraether lipids: a review, *Organic geochemistry*, 54, 19–61, 2013.
- Schrumpf, M. and Kaiser, K.: Large differences in estimates of soil organic carbon turnover in density fractions by using single and repeated radiocarbon inventories, *Geoderma*, 239, 168–178, 2015.
- 505 Shah, S. R. and Pearson, A.: Ultra-microscale (5–25  $\mu\text{g C}$ ) analysis of individual lipids by  $^{14}\text{C}$  AMS: Assessment and correction for sample processing blanks, *Radiocarbon*, 49, 69–82, 2007.
- Shah, S. R., Mollenhauer, G., Ohkouchi, N., Eglinton, T. I., and Pearson, A.: Origins of archaeal tetraether lipids in sediments: Insights from radiocarbon analysis, *Geochimica et Cosmochimica Acta*, 72, 4577–4594, 2008.
- Smittenberg, R. H., Hopmans, E. C., Schouten, S., and Damsté, J. S. S.: Rapid isolation of biomarkers for compound specific radiocar- 510 bon dating using high-performance liquid chromatography and flow injection analysis—atmospheric pressure chemical ionisation mass spectrometry, *Journal of Chromatography A*, 978, 129–140, 2002.



- Smittenberg, R. H., Hopmans, E. C., Schouten, S., Hayes, J. M., Eglinton, T. I., and Sinninghe Damste, J. S.: Compound-specific radiocarbon dating of the varved Holocene sedimentary record of Saanich Inlet, Canada, *Paleoceanography*, 19, 2004.
- 515 Smittenberg, R. H., Baas, M., Green, M. J., Hopmans, E. C., Schouten, S., and Damsté, J. S.: Pre-and post-industrial environmental changes as revealed by the biogeochemical sedimentary record of Drammensfjord, Norway, *Marine Geology*, 214, 177–200, 2005.
- Solly, E. F., Brunner, I., Helmisaari, H.-S., Herzog, C., Leppälammil-Kujansuu, J., Schöning, I., Schruppf, M., Schweingruber, F. H., Trumbore, S. E., and Hagedorn, F.: Unravelling the age of fine roots of temperate and boreal forests, *Nature communications*, 9, 1–8, 2018.
- Synal, H., Stocker, M., and Suter, M.: Nuclear Instruments & Methods in Physics Research Section B-Beam 389, *Interactions with Materials and Atoms*, 259, 7–13, 2007.
- 520 Tao, S., Eglinton, T. I., Montluçon, D. B., McIntyre, C., and Zhao, M.: Pre-aged soil organic carbon as a major component of the Yellow River suspended load: Regional significance and global relevance, *Earth and Planetary Science Letters*, 414, 77–86, 2015.
- Torn, M., Swanston, C., Castanha, C., and Trumbore, S.: Storage and turnover of organic matter in soil, *Biophysico-chemical processes involving natural nonliving organic matter in environmental systems*. Wiley, Hoboken, pp. 219–272, 2009.
- Trumbore, S. E., Chadwick, O. A., and Amundson, R.: Rapid exchange between soil carbon and atmospheric carbon dioxide driven by  
525 temperature change, *Science*, 272, 393–396, 1996.
- Tunlid, A. and White, D. C.: *Biochemical Analysis Of Biomass, Community Structure, Nutritional Status, and Metabolic Activity*, *Soil biochemistry*, 7, 229, 1991.
- Urich, T., Lanzén, A., Qi, J., Huson, D. H., Schleper, C., and Schuster, S. C.: Simultaneous assessment of soil microbial community structure and function through analysis of the meta-transcriptome, *PloS one*, 3, 2008.
- 530 Van der Voort, T. S., Zell, C., Hagedorn, F., Feng, X., McIntyre, C. P., Haghypour, N., Graf Pannatier, E., and Eglinton, T. I.: Diverse soil carbon dynamics expressed at the molecular level, *Geophysical Research Letters*, 44, 11–840, 2017.
- van der Voort, T. S., Mannu, U., Hagedorn, F., McIntyre, C., Walthert, L., Schleppe, P., Haghypour, N., and Eglinton, T. I.: Dynamics of deep soil carbon—insights from 14C time series across a climatic gradient, *Biogeosciences*, 16, 3233–3246, 2019.
- van der Voort, T. S. v. d., Hagedorn, F., McIntyre, C., Zell, C., Walthert, L., Schleppe, P., Feng, X., and Eglinton, T. I.: Variability in 14 C  
535 contents of soil organic matter at the plot and regional scale across climatic and geologic gradients, *Biogeosciences*, 13, 3427–3439, 2016.
- von Lützow, M., Kögel-Knabner, I., Ludwig, B., Matzner, E., Flessa, H., Ekschmitt, K., Guggenberger, G., Marschner, B., and Kalbitz, K.: Stabilization mechanisms of organic matter in four temperate soils: Development and application of a conceptual model, *Journal of Plant Nutrition and Soil Science*, 171, 111–124, 2008.
- Vonk, J. E., Drenzek, N. J., Huguen, K. A., Stanley, R. H., McIntyre, C., Montluçon, D. B., Giosan, L., Southon, J. R., Santos, G. M.,  
540 Druffel, E. R., et al.: Temporal deconvolution of vascular plant-derived fatty acids exported from terrestrial watersheds, *Geochimica et Cosmochimica Acta*, 244, 502–521, 2019.
- Walthert, L.: *Langfristige Waldökosystem-Forschung LWF in der Schweiz, Kernprojekt Bodenmatrix: Ergebnisse der ersten Erhebung 1994–1999*, Tech. rep., ETH Zurich, 2003.
- Weber, Y., De Jonge, C., Rijpstra, W. I. C., Hopmans, E. C., Stadnitskaia, A., Schubert, C. J., Lehmann, M. F., Damste, J. S. S., and Niemann,  
545 H.: Identification and carbon isotope composition of a novel branched GDGT isomer in lake sediments: Evidence for lacustrine branched GDGT production, *Geochimica et Cosmochimica Acta*, 154, 118–129, 2015.
- Weijers, J., Wiesenberg, G., Bol, R., Hopmans, E., and Pancost, R.: Carbon isotopic composition of branched tetraether membrane lipids in soils suggest a rapid turnover and a heterotrophic life style of their source organism (s), *Biogeosciences*, 7, 2959–2973, 2010.



- 550 Weijers, J. W., Schouten, S., Hopmans, E. C., Geenevasen, J. A., David, O. R., Coleman, J. M., Pancost, R. D., and Sinninghe Damsté, J. S.:  
Membrane lipids of mesophilic anaerobic bacteria thriving in peats have typical archaeal traits, *Environmental Microbiology*, 8, 648–657,  
2006a.
- Weijers, J. W., Schouten, S., Spaargaren, O. C., and Damsté, J. S. S.: Occurrence and distribution of tetraether membrane lipids in soils:  
Implications for the use of the TEX86 proxy and the BIT index, *Organic Geochemistry*, 37, 1680–1693, 2006b.
- 555 Weijers, J. W., Schouten, S., van den Donker, J. C., Hopmans, E. C., and Damsté, J. S. S.: Environmental controls on bacterial tetraether  
membrane lipid distribution in soils, *Geochimica et Cosmochimica Acta*, 71, 703–713, 2007.
- Yamamoto, Y., Ajioka, T., and Yamamoto, M.: Climate reconstruction based on GDGT-based proxies in a paleosol sequence in Japan:  
Postdepositional effect on the estimation of air temperature, *Quaternary international*, 397, 380–391, 2016.
- Yang, H., Pancost, R. D., Jia, C., and Xie, S.: The response of archaeal tetraether membrane lipids in surface soils to temperature: a potential  
paleothermometer in paleosols, *Geomicrobiology Journal*, 33, 98–109, 2016.
- 560 Zimmermann, S., Luster, J., Blaser, P., Walthert, L., and Lüscher, P.: *Waldböden der Schweiz, Band 3, Regionen Mittelland und Voralpen*,  
Swiss Federal Research Institute WSL, Hep Verlag Bern, Switzerland, 2006.

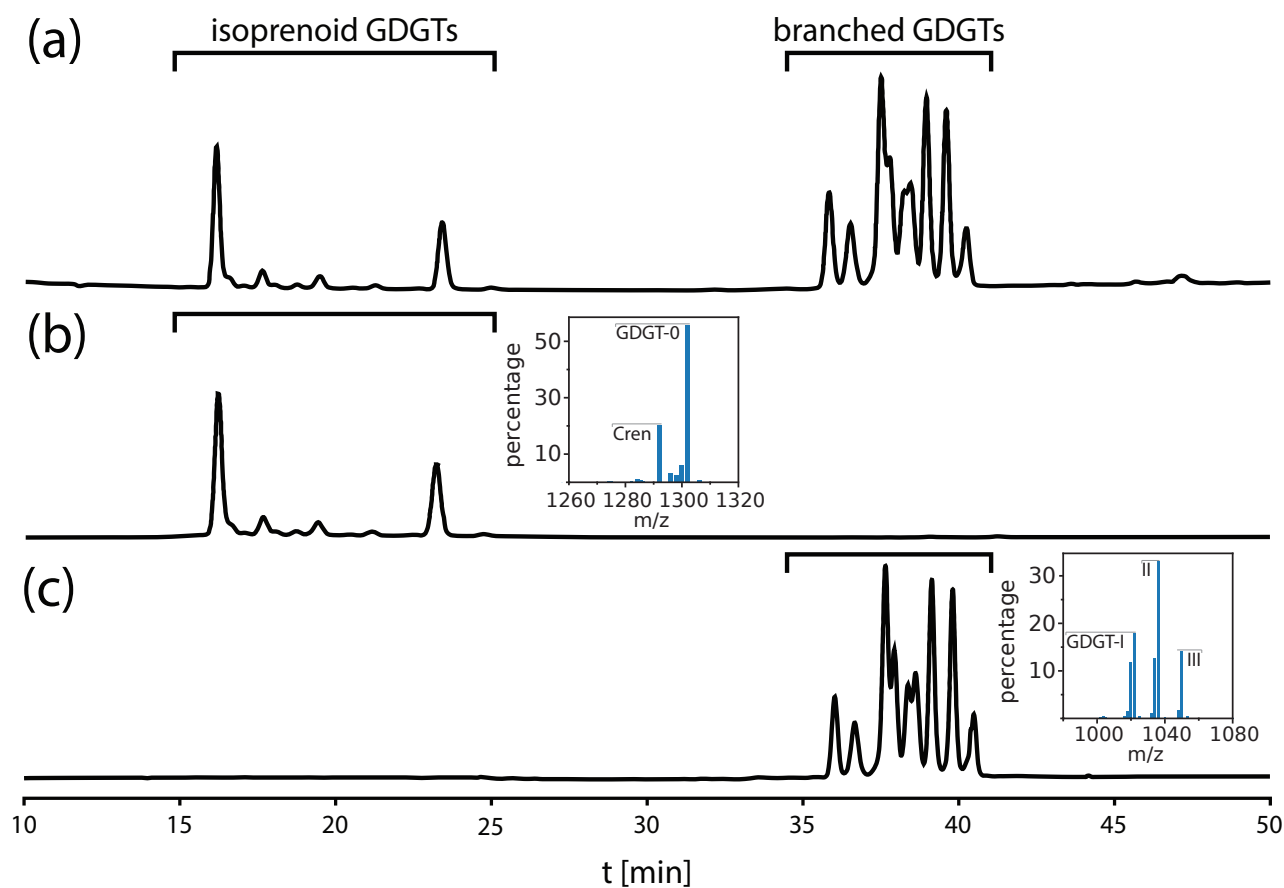


**Figure 1.** HPLC mass chromatograms ( $m/z$  500 - 1500) of GDGTs from a composition topsoil sample. a) sample before GDGT isolation, b) the separated isoprenoid fraction and its composite mass spectrum (GDGT-3, GDGT-2 and GDGT-1 from left to right between Crenarcheol (Cren) and GDGT-0 are not labelled), c) the separated branched fraction and its composite mass spectrum (GDGT-I, II and III, corresponding to tetra-, penta- and hexamethylated GDGTs are labelled)(For molecular structures see Figure A1)

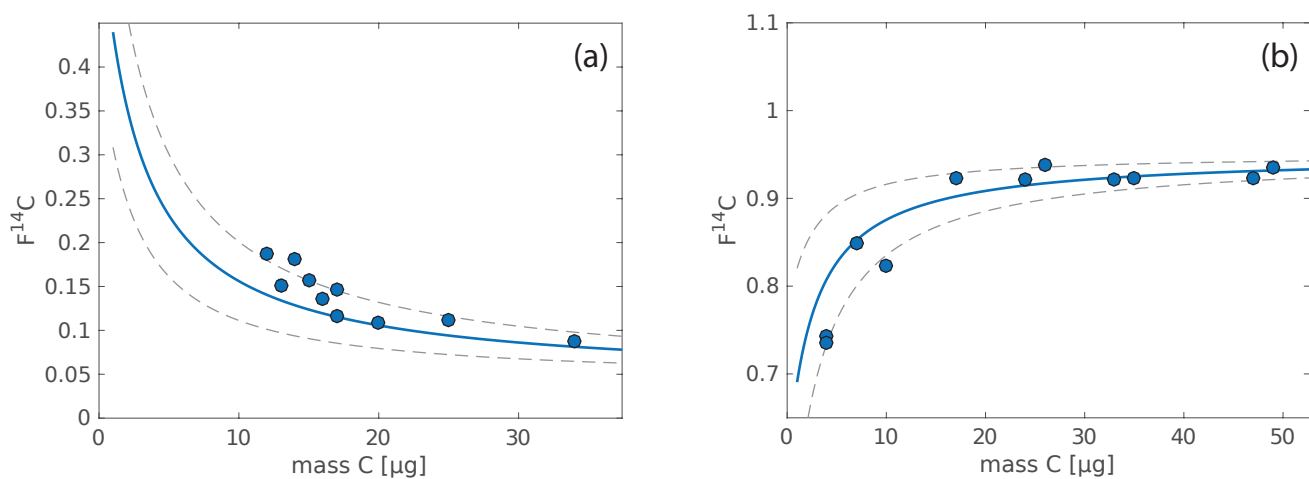


**Figure 2. Blank assessment associated with GDGT isolation.** a) The  $F^{14}\text{C}$  dead standard (lignite) tracing a modern constant contamination of  $1.55 \mu\text{g C}$ , b) The  $F^{14}\text{C}$  modern standard (topsoil composite) tracing a radiocarbon dead constant contamination of  $1.07 \mu\text{g C}$ . The solid line indicates the best fit of contamination mass and radiocarbon signal for both sets of samples considered jointly, the grey dotted lines show the  $1\sigma$  error range

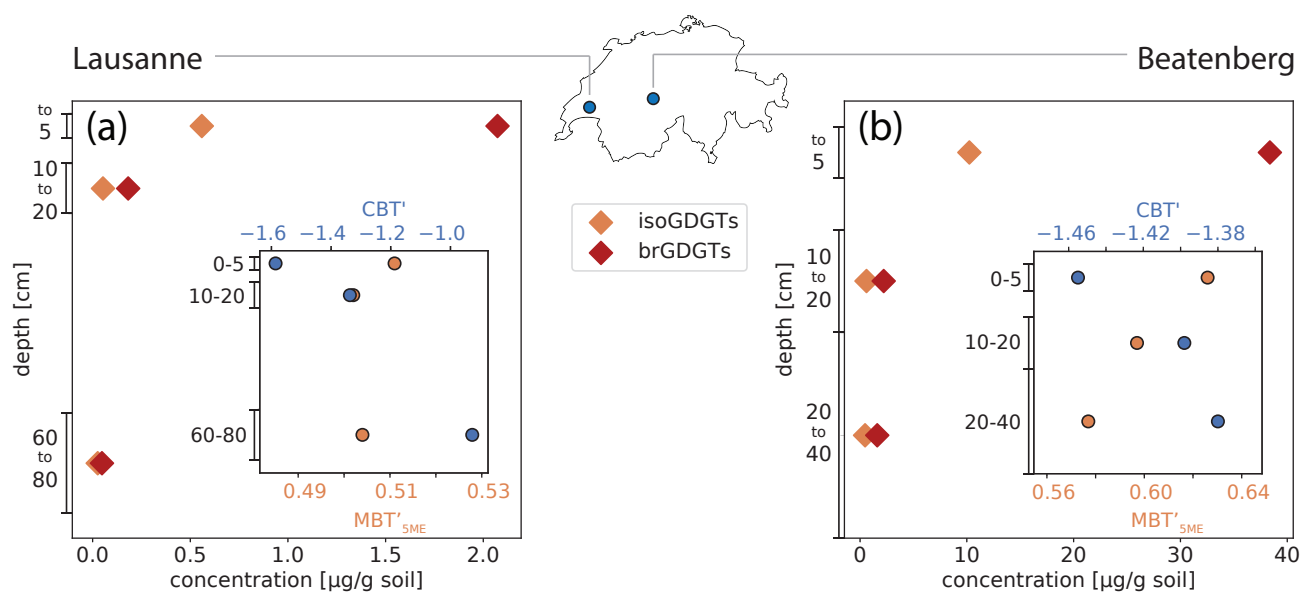


**Figure 3. BrGDGT abundances and parameter ratios in Lausanne and Beatenberg soil profiles.** In both soils (a - Lausanne, b - Beatenberg) the concentration of the samples per dry weight decreases rapidly with depth. The inner plots show the brGDGT-derived MBT'<sub>5ME</sub> (orange) and the CBT' (blue) indices in the respective soil. While the MBT'<sub>5ME</sub> does not vary a lot with depth, the CBT' increases significantly with depth in the Lausanne soil.

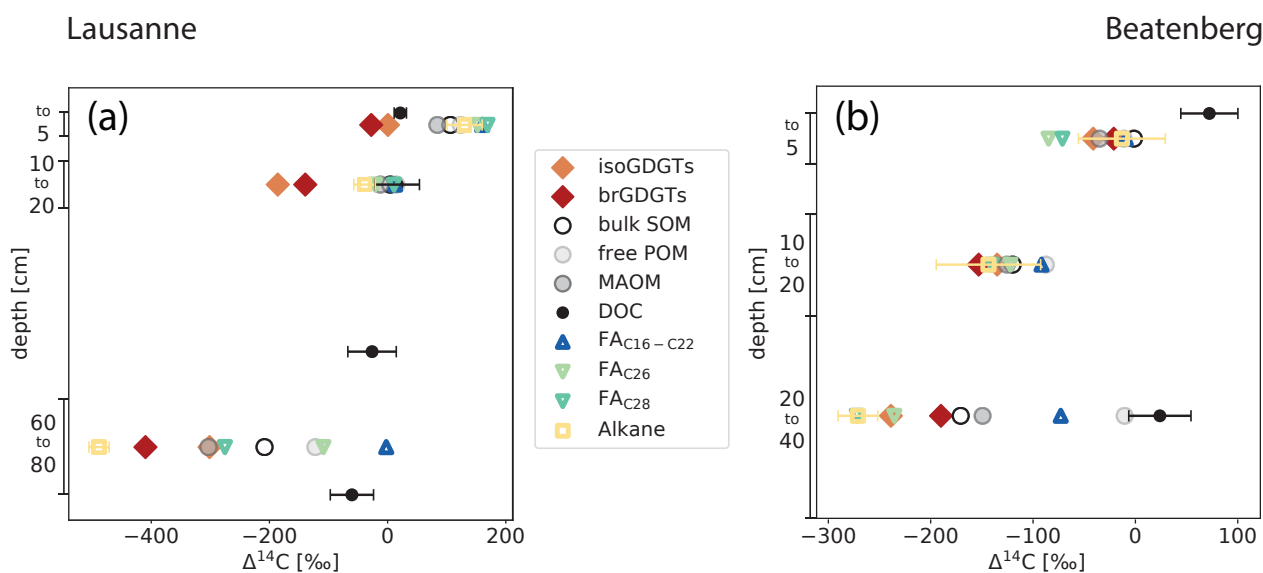


**Figure 4. Radiocarbon content, expressed as  $\Delta^{14}\text{C}$  of organic matter fractions and compounds in Lausanne and Beatenberg soil profiles.** In both soils (Lausanne - A, Beatenberg - B) the radiocarbon contents of both branched and isoprenoid GDGTs decrease to a similar degree to that of bulk SOM in each profile. The measured n-alkane in the Beatenberg soil is  $\text{C}_{29}$ , in the Lausanne soil the n- $\text{C}_{27}$  homologue was analyzed. Alkane, n-fatty acid (FA), free particulate organic matter (POM), mineral-associated organic matter (MAOM) and dissolved organic carbon (DOC)  $\Delta^{14}\text{C}$  values are taken from Van der Voort et al. (2017). DOC was not measured in the same intervals as the other parameters, but at 0, 15, 50 and 80 cm, and at 0 and 30 cm depth in the Lausanne and Beatenberg soils, respectively. If error bars are not visible, then the uncertainty is smaller than the symbol size.

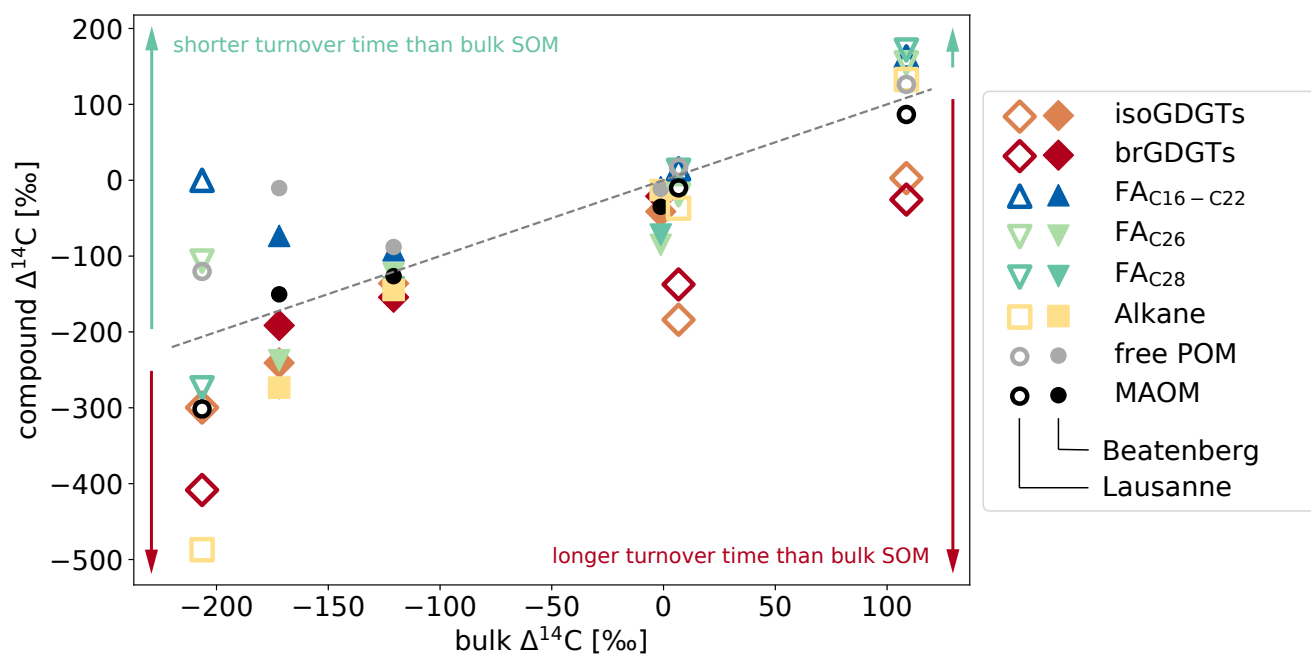


**Figure 5. Relationship between  $\Delta^{14}\text{C}$  values of specific components and bulk SOM in Beatenberg and Lausanne soil profiles.** The different analyzed compounds and density fractions (Van der Voort et al., 2017) cover a greater range of  $\Delta^{14}\text{C}$  values with soil depth as reflected in the ageing of the bulk OC in the respective soil. The dotted line represents equal compound and bulk  $\Delta^{14}\text{C}$ . Two groups are discernable: those with  $\Delta^{14}\text{C}$  values higher than the bulk OC, and thus with a more rapid turnover (in most samples, this includes short-chain (C<sub>16</sub>-C<sub>22</sub>) FA and the low density fraction (free POM) and those with lower  $\Delta^{14}\text{C}$  values implying longer turnover times (including long-chain n-alkanes (in the Beatenberg soil C<sub>29</sub>-alkane, in the Lausanne soil the C<sub>27</sub>), and fatty acids (C<sub>26</sub>, C<sub>28</sub> FA) and the GDGTs.



**Table 1. Turnover times of isoprenoid and branched GDGTs.** Turnover times are based on the single-pool turnover time of the light fraction (fPOM) or the short-chain fatty acids (SCFA - in brackets) as approximation of the fast pool.

loc	depth	fast pool proportion	turnover times fPOM (SCFA) [years]					
			fast pool		isoGDGT		brGDGT	
Bb	0-5cm	0.897	350	(340)	710	(740)	440	(450)
	10-20cm	0.193	890	(920)	1400	(1400)	1600	(1600)
	20-40cm	0.115	350	(760)	2800	(2700)	2100	(2000)
Ln	0-5cm	0.162	46	(33)	350	(360)	540	(550)
	10-20cm	0.113	240	(240)	2000	(2000)	1400	(1400)
	60-80cm	0.087	1200	(300)	3600	(3700)	5900	(6100)



**Table 2. Soil properties related to the stability of soil organic matter.** CEC (effective cation exchange capacity),  $Fe_d$  (dithionite-extractable iron),  $Fe_o$  and  $Al_o$  (oxalate-extractable iron and aluminum),  $Fe_p$  and  $Al_p$  (pyrophosphate-extractable iron and aluminum) as well as sand, silt and clay content are provided by Zimmermann et al. (2006)

loc	depth	CEC [mmolC kg <sup>-1</sup> ]	$Fe_d$ [ppm]	$Fe_o$ [ppm]	$Fe_p$ [ppm]	$Al_o$ [ppm]	$Al_p$ [ppm]	sand [%]	silt [%]	clay [%]
Bb	0-5cm	50	1047	684	505	538	571	84	7	8
	10-20cm	15	na	133	99	280	268	83	15	3
	20-40cm	37	5770	2183	2062	880	1713	80	14	6
Ln	0-5cm	77	6187	3356	2900	1861	1304	62	25	13
	10-20cm	61	6493	3039	2310	2030	1430	51	31	18
	60-80cm	59	5840	2095	732	1156	791	57	27	16



isoprenoid GDGTs

Name	m/z
Crenarchaeol	1292
Crenarchaeol'	1292'
GDGT - 0	1302
GDGT - 1	1300
GDGT - 2	1298
GDGT - 3	1296

branched GDGTs

Name	6-methyl isomer	m/z
Ia		1022
Ib		1020
Ic		1018
IIa / IIa'		1036
IIb / IIb'		1034
IIc / IIc'		1032
IIIa / IIIa'		1050
IIIb / IIIb'		1048
IIIc / IIIc'		1046

Figure A1. Molecular structures of GDGTs analyzed in this study